

GA-A27933

**TURBULENCE BEHAVIOR AND
TRANSPORT RESPONSE APPROACHING
BURNING PLASMA RELEVANT PARAMETERS**

by

**G.R. McKEE, C. HOLLAND, Z. YAN, E.J. DOYLE, T.C. LUCE, A. MARINONI,
C.C. PETTY, T.L. RHODES, J.C. ROST, L. SCHMITZ, W.M. SOLOMON, B.J. TOBIAS,
G. WANG, and L. ZENG**

SEPTEMBER 2014



DISCLAIMER

This report was prepared as an account of work sponsored by an agency of the United States Government. Neither the United States Government nor any agency thereof, nor any of their employees, makes any warranty, express or implied, or assumes any legal liability or responsibility for the accuracy, completeness, or usefulness of any information, apparatus, product, or process disclosed, or represents that its use would not infringe privately owned rights. Reference herein to any specific commercial product, process, or service by trade name, trademark, manufacturer, or otherwise, does not necessarily constitute or imply its endorsement, recommendation, or favoring by the United States Government or any agency thereof. The views and opinions of authors expressed herein do not necessarily state or reflect those of the United States Government or any agency thereof.

TURBULENCE BEHAVIOR AND TRANSPORT RESPONSE APPROACHING BURNING PLASMA RELEVANT PARAMETERS

by

G.R. McKEE,^{*} C. HOLLAND,[†] Z. YAN,^{*} E.J. DOYLE,[‡] T.C. LUCE, A. MARINONI,[¶]
C.C. PETTY, T.L. RHODES,[‡] J.C. ROST,[#] L. SCHMITZ,[‡] W.M. SOLOMON,[§] B.J. TOBIAS,[§]
G. WANG,[‡] and L. ZENG[‡]

This is a preprint of a paper to be presented at the Twenty-Fifth IAEA Fusion Energy Conf., October 13-18, 2014 in Saint Petersburg, Russia, and to be published in the *Proceedings*.

^{*}University of Wisconsin-Madison, Madison, Wisconsin.

[†]University of California San Diego, La Jolla, California.

[‡]University of California Los Angeles, Los Angeles, California.

[¶]Massachusetts Institute of Technology, Cambridge, Massachusetts.

[#]Massachusetts Institute of Technology, Cambridge, Massachusetts.

[§]Princeton Plasma Physics Laboratory, Princeton, New Jersey.

Work supported by
the U.S. Department of Energy
under DE-FG02-89ER53296, DE-FG02-08ER54999,
DE-FG02-06ER54871, DE-FG02-08ER54984, DE-FC02-04ER54698,
DE-FG02-04ER54235, and DE-AC02-09CH11466

GENERAL ATOMICS PROJECT 30200
SEPTEMBER 2014



Turbulence Behavior and Transport Response Approaching Burning Plasma Relevant Parameters

G.R. McKee¹, C. Holland², Z. Yan¹, E.J. Doyle³, T.C. Luce⁴, A. Marinoni⁵, C.C. Petty⁴, T.L. Rhodes³, J.C. Rost⁵, L. Schmitz³, W.M. Solomon⁶, B.J. Tobias⁶, G. Wang³, and L. Zeng³

¹University of Wisconsin-Madison, 1500 Engineering Dr., Madison, WI 53706-1687, USA

²University of California San Diego, 9500 Gilman Dr., La Jolla, CA 92093-0417, USA

³University of California Los Angeles, PO Box 957099, Los Angeles, CA 90095-7099, USA

⁴General Atomics, PO Box 85608, San Diego, CA 92186-5608, USA

⁵Massachusetts Institute of Technology, Cambridge, MA 02139, USA

⁶Princeton Plasma Physics Laboratory, PO Box 451, Princeton, NJ 08543-0451, USA

E-mail contact of main author: mckee@fusion.gat.com

Abstract. Multi-scale turbulence properties are significantly altered in high-beta advanced inductive plasmas as parameters approach those anticipated in burning plasmas, in particular lower toroidal rotation and near unity T_e/T_i . Fluctuations are observed to increase by multiple diagnostics in H-mode plasmas on DIII-D as rotation is lowered and T_e/T_i increases, explaining the consequent local transport increases and global energy confinement time reduction. The energy confinement time is reduced by about 40% as the toroidal rotation is decreased by nearly a factor of three, while core turbulence increases in matched advanced-inductive plasmas ($\beta_e \approx 2.7$, $q_{95} = 5.1$). Density, electron and ion temperature profiles, as well as relevant dimensionless parameters (β , ρ^* , q_{95} , T_e/T_i , and v^*) were maintained nearly fixed. Low-wavenumber (ion gyroradius scale) density fluctuations measured with beam emission spectroscopy near mid-radius show significant amplitude reduction, while fluctuations in the outer region of the plasma ($\rho > 0.6$) exhibit little change in amplitude. Intermediate to high wavenumber fluctuations measured with Doppler backscattering and phase contrast imaging exhibit a similar decreasing trend at higher rotation. Linear GYRO calculations are broadly consistent since localized ω_{ExB} shearing rates exceed growth rates in this mid-radial zone where fluctuations are suppressed at high rotation, while this relationship is reversed at lower rotation where ω_{ExB} shearing rates are well below local growth rates; calculated temperature and density profiles with TGLF are similar to experimental measurements. When the T_e/T_i ratio approaches unity via off-axis electron cyclotron heating, low-k density fluctuations are observed to increase over the radial range $0.3 < \rho < 0.8$ as particle, thermal and momentum transport increases. The spatial correlation properties are slightly modified, suggesting a change in the dominant underlying instability driving the observed fluctuations. The energy confinement time is correspondingly reduced by 30%. GYRO calculations indicate increases in linear growth rates and quasi-linear fluxes that are consistent with these observed changes; TGLF also reasonably accurately reproduces the expected kinetic profiles.

1. Introduction

Transport in burning plasmas will exhibit significantly different characteristics and parametric dependencies compared with that in modern tokamak experiments, and so it is crucial to test transport models and validate simulations in regimes that more closely approach burning plasma conditions in order to gain confidence in the predicted energy and particle confinement and thus overall performance. Burning plasmas, such as ITER, will naturally have substantial electron heating from slowing alpha particles, collisionally coupled electrons and ions, and equilibrated electron, ion and impurity temperatures, while collisionality ($\nu = \nu_{ie}/\omega_B$) will be relatively low at high Greenwald density fraction. In addition, the applied toroidal torque from beams or intrinsic sources is expected to be relatively low compared with plasma rotational inertia and thus toroidal rotation and radially averaged ExB shearing rates are expected to be low, while growth rates of gradient-driven turbulence will be similar on average to contemporary experiments. Understanding how relevant dimensionless parameters such as ρ^* , T_e/T_i , $\gamma_{\text{lin}}/\omega_{\text{ExB}}$, ν , q_{95} , β_N , and impurity fraction, impact turbulence and the resulting transport as burning plasma conditions are approached is thus important to accurately predicting burning plasma performance. These

parameters impact growth rates and alter which instabilities, such as ion and electron temperature gradient-driven, microtearing, and trapped electron modes, drive fluctuations and thus determine the saturated turbulence state as well as thermal and particle transport characteristics.

In the experiments described here, toroidal rotation and T_e/T_i are systematically varied in high normalized-pressure H-mode plasmas while other critical dimensionless parameter profiles and gradients are held nearly constant. To perform these experiments, it was critical to employ the co-current and counter-current neutral beam injection systems [1], high-power electron cyclotron heating (ECH), suite of advanced fluctuation diagnostics and high-performance scenarios on DIII-D. Fluctuation measurements were obtained with beam emission spectroscopy (BES) (low-k density fluctuations), Doppler backscattering (DBS) (intermediate-k density fluctuations), and phase contrast imaging (PCI) (low to high-k density fluctuations) to obtain multiscale fluctuation measurements over the wavenumber range for expected instabilities that drive thermal transport. In order to assess the fidelity of current transport models in accurately predicting the plasma density and temperature profiles and their responses to changes in applied heating and torque, predictions of core kinetic profiles made using the quasilinear TGLF transport model [2] are compared to the experimental measurements; comparisons to nonlinear gyrokinetic simulations will be reported in future work. As a first step in understanding the observed changes in fluctuation amplitudes, the results of linear gyrokinetic growth rate calculations are compared with observed responses in fluctuation spectra and amplitudes.

To understand how transport behaves approaching anticipated burning plasma conditions, advanced inductive (hybrid) plasmas were employed to achieve relatively high normalized pressure (β_N) with good confinement ($1 < H_{98} < 1.5$.) Advanced-inductive plasmas exhibit several additional advantageous features for performing transport experiments and analysis: long-duration ($\tau_{\text{DURATION}}/\tau_E > 20$), steady parameters, sawtooth-free conditions, and robust, reproducible operation over a wide parameter range; repeat discharges were run to obtain fluctuation measurements over a wide radial and wavenumber range. Typically, a benign $m/n=3/2$ tearing mode develops that prevents q_{min} from falling below 1 [3]. The long-pulse discharges benefit fluctuation analysis since turbulence amplitudes in these high confinement discharges are quite low ($\tilde{n}/n \ll 1\%$ throughout high gradient regions at mid-radii); the long duration allows for ensemble-averaging of spectral and correlation characteristics over long time windows, thus increasing signal-to-noise in the extracted small-scale fluctuations. Several dimensionless parameters for the rotation and T_e/T_i scans are compared in Table I.

TABLE I. DIMENSIONLESS PARAMETERS

Parameter	Low V_{TOR}	High V_{TOR}	Low T_e/T_i	High T_e/T_i
Mach #	0.18	0.5	0.2	0.2
$T_e/T_i(0)$	0.5	0.5	0.5	0.9
ρ^*	0.016	0.016	0.016	0.016
β_N	2.7	2.7	2.45	2.45
q_{95}	5.1	5.1	5.8	5.8
$\tau_r(\text{ms})$	105	148	115	75
$H_{98y,2}$	1.36	(na)	1.27	1.13
DIII-D Shot	155583	155575	142019	142011

2. Turbulence and Transport Variation with Toroidal Rotation and Shear

The core toroidal rotation was varied by over a factor of two in otherwise well-matched advanced-inductive plasmas ($I_p=1.2$ MA, $B_1=1.9$ T, $\beta_s \approx 2.7$, $q_{95}=5.1$) while dimensionless parameters (β , ρ^* , q_{95} , T_e/T_i , and v^*) and temperature and density profiles are held nearly fixed. The core Mach number, M ($=V_{\text{TOR}}/V_{\text{TH,I}}$), varied from $M_0=0.2$ to nearly $M_0=0.5$. Stored energy and density were held fixed via the Plasma Control System; neutral beam power was adjusted up or down as necessary as confinement varied with rotation. ExB shear profiles [4] changed significantly with rotation, with a profile-averaged increase in shearing rate at higher rotation.

Further reduction in toroidal rotation led to the onset of $m/n=2/1$ neoclassical tearing modes (NTMs), which were avoided for this transport analysis. Related experiments were performed previously [5], although fluctuation measurements were not available. The global energy confinement time increases by 40% from low to high rotation.

2.1. Measured and TGLF-predicted kinetic profiles

The toroidal rotation profiles measured with charge exchange recombination spectroscopy are shown in Fig. 1(a) for the two cases. Experimentally measured profiles of ion and electron temperature and density at high and low rotation are compared with profiles predicted by the TGLF transport model [2] in Fig. 1(b-d). The experimental ion temperature profiles are broadly similar, however, a significant 10% reduction in the measured ion temperature at low rotation, relative to the high rotation case, is evident at mid-radius. This difference is outside of the experimental uncertainty and reflects increased ion thermal transport at lower rotation. The electron temperature profile [Fig. 1(c)] is somewhat higher at higher rotation, consistent with transport modifications, and also exhibits a flat structure near $\rho=0.35$ that likely results from the benign $3/2$ mode. Note the rotation profile [Fig. 1(a)] also shows a local flattening near the same radius. Why the $3/2$ mode leads to such significant changes in V_{tor} and T_e gradients at high, but not low, rotation, remains undetermined.

The TGLF model is used to calculate self-consistent temperature and density profiles from independently calculated power and particle sources via the NUBEAM module, rotation (and shear) profile, magnetic geometry, and boundary conditions (profiles match data at $\rho=0.8$.) Flux-matched simulations were performed using the TGYRO code so that calculated profile gradients drive the necessary thermal and particle transport to match experimental fluxes. The resulting calculated profiles for high and low rotation were compared to measurements in Fig. 1. The calculated ion temperature profiles match generally well, though

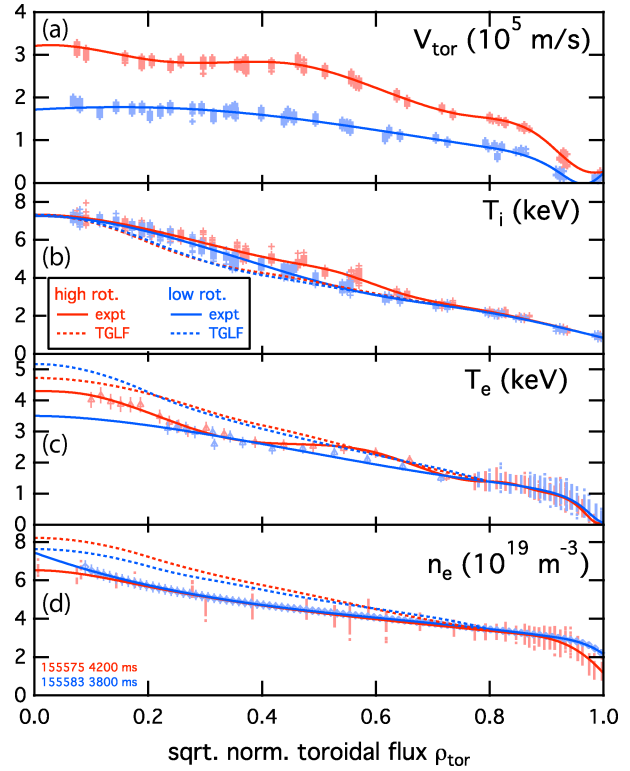


Fig. 1. Comparison of profiles in high (red) and low (blue) rotation (solid: experiment; dashed: TGLF); (a) Toroidal vel. (CER); (b) T_i (CER), (c) T_e (ECE/TS), (d) n_e (Refl./TS).

mid-radial T_i is slightly under-predicted, while the T_e and n_e profiles are correspondingly over-predicted. This may result partially from the 3/2 mode near $\rho=0.4$. The electron temperature is significantly lower than ion temperature in these neutral beam-heated discharges, which results in significant electron-ion collisional exchange, such that the power balance analysis indicates electron thermal transport dominates the ions. However, linear analysis (discussed further in Sec. 2.3) indicates that the ion temperature gradient (ITG) mode (which tends to drive equal amounts of ion and electron thermal transport) is the dominant instability at low k in such both plasmas. This imbalance leads to the increased T_e and n_e predictions, with the predicted steady-state profiles having reduced collisional exchange (self-consistently calculated in TGYRO) and roughly equal ion and electron thermal fluxes. Both Thomson scattering and electron cyclotron emission (ECE) measurements are employed in the fits. Electron density profiles are measured with the reflectometer and Thomson scattering, which are largely in agreement and show a good density match.

2.2 Variation of turbulence characteristics with rotation

Core density fluctuations were measured over the range $0.5 < k_{\perp} < 10 \text{ cm}^{-1}$ with BES [6] at low- k , DBS [7] at intermediate- k , and PCI [8] at low to high- k . The fluctuation spectra at two radial locations from BES are compared in Fig. 2(a) and 2(b) for high and low-rotation plasmas. At $\rho=0.5$, a broad fluctuation spectrum is observed at low rotation, peaking near 230 kHz ($k_{\perp}\rho_s \approx 0.3$), while fluctuations are largely suppressed in the high rotation discharge. In contrast, similar amplitude spectra are obtained for both high and low rotation at $\rho=0.75$. The shift in the peak frequency of the spectra from about 160 kHz to 240 kHz is explained by the change in the measured fluctuation poloidal velocity. Figure 2(c) compares the amplitude profile for the two rotation conditions. The fluctuation amplitudes are rather similar over much of the outer core region ($\rho > 0.55$); the main differences arise at and inside of $\rho=0.55$, where a clear reduction in fluctuation amplitude is observed in the high rotation plasmas. Higher toroidal rotation leads to higher ExB shear and turbulence suppression, but this is a radially localized effect.

Figure 2(d) compares the poloidal velocity of density fluctuations measured with BES to the ExB velocity obtained with charge exchange recombina-

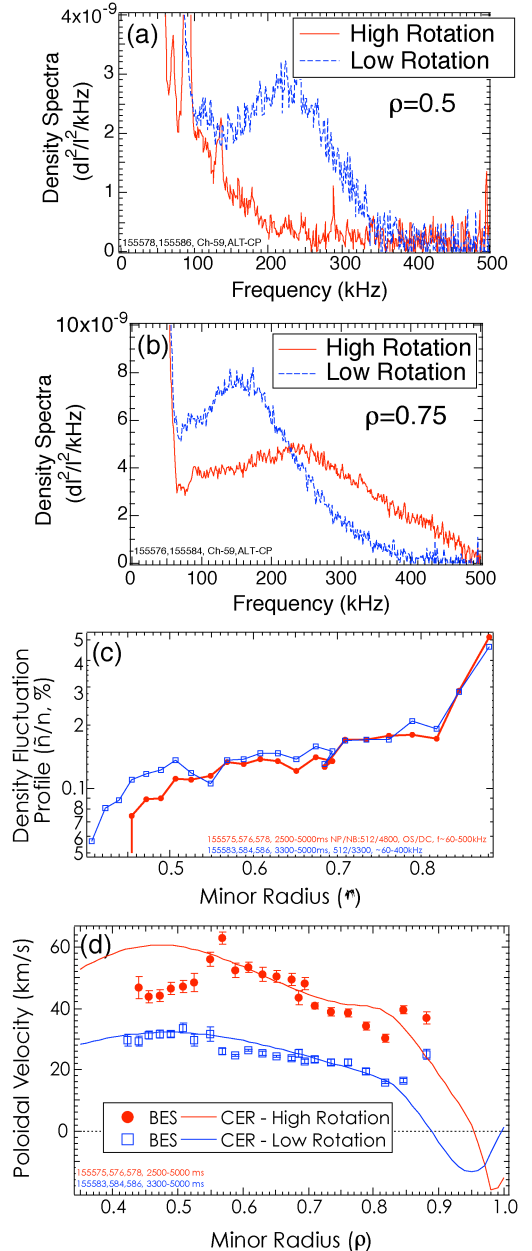


Fig. 2. Low-wavenumber density fluctuation measurements from BES in high and low rotation discharges over 3 repeated discharges each: (a) spectra at $\rho=0.5$, (b) spectra at $\rho=0.75$, (c) amplitude profile (log scale), (d) poloidal ExB velocity from BES (points) and CER (curve).

ation (CER) measurements. The BES measurements were obtained via time-lag cross-correlation between the multiple poloidally-displaced channels in the 2D array. The measured E_r profile comes from a radial force balance analysis that uses CER measurements of the carbon ion pressure, toroidal rotation, poloidal rotation, and the local magnetic field (from an EFIT reconstruction which uses both measured pressure and current [via motional Stark effect (MSE) as constraints]). The close agreement reflects consistency between the independent measurements and indicates that the propagation of fluctuations in the plasma frame is small compared with the ExB velocity. This is similar to observations obtained in a set of L-mode plasmas [9,10] employed for validation studies. While the velocities compare well over much of the profile, a notable deviation occurs at high and low rotation towards the outer radial zone, with the turbulence velocity higher in magnitude than the ExB velocity; this difference may reflect turbulence advection in the ion diamagnetic direction in the plasma frame; a similar observation was made in the outer radial regions of L-mode discharges [9].

Low-to-high wavenumber fluctuations from PCI are compared for high and low rotation in Fig. 3(a). PCI measures the spatially integrated fluctuations along a vertical chord located at $R=194-202$ cm, ($\rho \geq 0.3$). Fluctuations are Doppler-shifted at high rotation and the line-integrated fluctuation power is approximately 3 times higher at low rotation (note log-scale). In addition, the $m/n=3/2$ core tearing mode and harmonics are observed, which were not included in fluctuation power.

Intermediate-wavenumber fluctuations ($2.4 < k_{\perp} \rho_s < 3.6$) were measured with DBS and are compared in Fig. 3(b) near $\rho=0.7$ for the low and high rotation plasmas. These illustrate a change in Doppler shift and show a substantial reduction in integrated fluctuations at higher rotation. This result contrasts with the BES measurements at a similar radius, which indicated a similar magnitude of fluctuations, reflecting a wavenumber dependence to the suppression.

2.3 Linear growth rates calculations with GYRO

Calculated linear growth rates from GYRO are compared with shearing rates and qualitative aspects are compared to turbulence measurements. The growth rates are shown in Fig. 4 along with the corresponding ω_{ExB} shearing rates for the two radii at which spectra were displayed in Fig. 2(a) and 2(b). The calculations include electromagnetic effects ($dA_{\parallel} \neq 0$, $dB_{\parallel} = 0$), electron-ion collisions, and geometric effects through a generalized Miller representation.

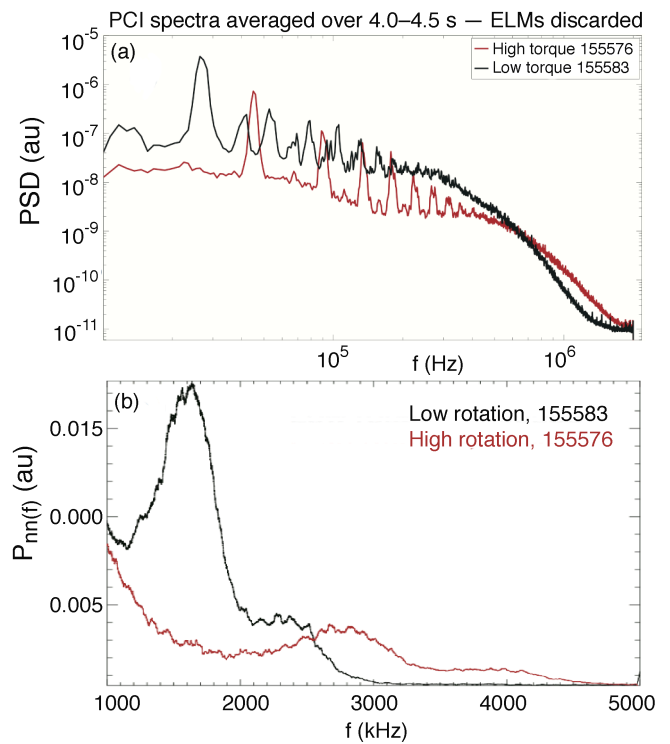


Fig. 3. Comparison of density fluctuation spectra at high and low rotation: (a) PCI (vertically line-averaged, low to high- k), and (b) DBS (intermediate- k_{\perp} , $\rho \sim 2.5-3.5$, $\rho=0.7$.)

At $\rho=0.75$, the growth rates exceed the shearing rates and are similar to each other. The growth rates peak close to where the fluctuation spectra peak, when frequency is converted to normalized poloidal wave number, $k_\theta \rho_s$, via the measured local poloidal velocity as $k_\theta = 2\pi f / v_\theta$ and $\rho_s = \sqrt{2T_e M_i} / eB$. Also, the peaks of both measured spectra and calculated growth rates are slightly downshifted in poloidal wavenumber at high rotation. At $\rho=0.5$, the high rotation plasma exhibits a low growth rate that is below the local shearing rate, and turbulence is correspondingly measured to be minimal (noise level), while at low rotation, the growth rate peak is comparable to the shearing rate and turbulence was much higher. Recall also from Fig. 1(b) that the T_i profile is somewhat higher at high rotation, consistent with lower growth rates and turbulent transport.

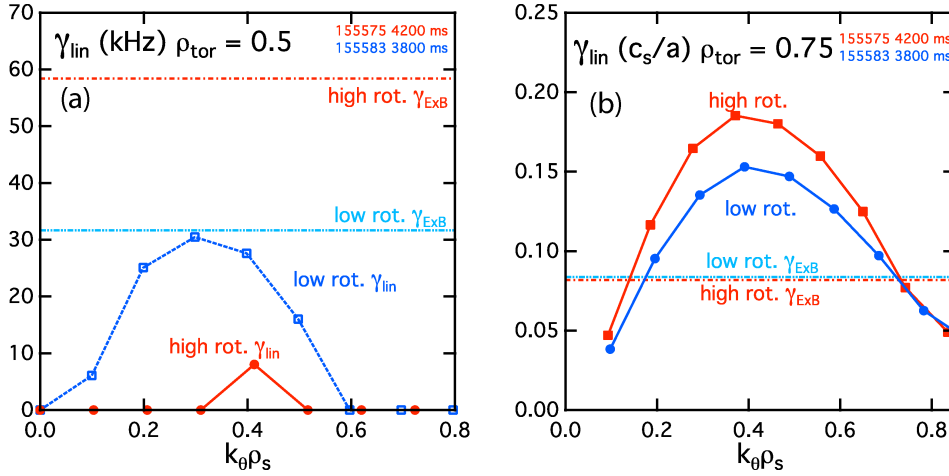


Fig. 4. Growth rates from GYRO compared with experimental ExB shearing rates from CER (E_r force balance) for (a) $\rho=0.5$ and (b) $\rho=0.75$.

3. Turbulence and Transport Variation with Electron to Ion Temperature Ratio

In related experiments that were also performed in advanced inductive discharges, the effects of the electron to ion temperature ratio, T_e/T_i where systematically investigated. It's been previously demonstrated that as the T_e/T_i ratio increases towards unity, transport increases and confinement is typically degraded [11,12]. Here, we relate fluctuation measurements, GYRO growth rates and profile predictions. The electron to ion temperature ratio was systematically increased by 25% via application of 3.5 MW of off-axis electron cyclotron heating, while core ion temperature and rotation were held fixed via feedback. The T_e profile is uniformly increased to maintain a similar electron temperature gradient scale length profile. Dimensionless parameters (β , ρ^* , q_{95} , M_o) are held nearly fixed as T_e/T_i is varied (collisionality also changed with T_e). Particle transport was increased at higher T_e/T_i .

Measured profiles for high and low T_e/T_i plasmas are compared in Fig. 5 with predicted profiles from TGLF. $T_i(0)$ is maintained nearly fixed, but the profiles do change modestly at mid radius as a result of increasing transport at higher T_e/T_i . TGLF most accurately reproduces the T_i profile at low T_e/T_i , but overestimates it at higher T_e/T_i . The electron temperature profiles increases uniformly by about 25% in the ECH-heated discharge, and TGLF flux-matched profiles are consistent. TGLF also over-predicts the density profile, particularly at low T_e/T_i ; this result is insensitive to uncertainties in the wall-recycling source.

Low-k density fluctuations were measured with BES over the radial range $0.3 < \rho < 0.8$ with the 2D array. Fluctuations are observed to increase as the T_e/T_i ratio is increased. The spectra, displayed in Figs. 6(a) and 6(b), indicate a fairly uniform increase as a function of

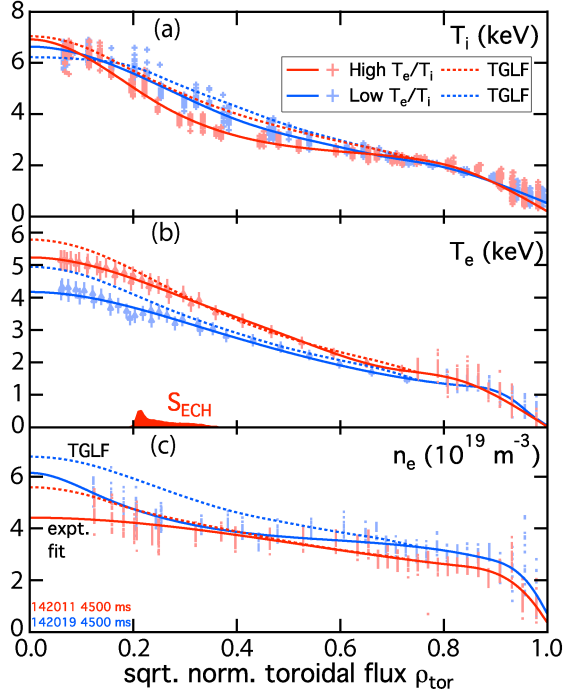


Fig. 5. Comparison of measured profiles at lower T_e/T_i (blue, solid) and higher T_e/T_i (red, solid) and TGLF calculated profiles (dashed) for: (a) electron temperature, (b) electron temperature, and (c) density.

frequency, which is nearly equivalent to poloidal wave-number. Figure 6(c) shows the amplitude profile, which shows a relatively uniform increase across the profile, unlike in the rotation experiments. Commensurate with this fluctuation amplitude increase with T_e/T_i , transport increases in all channels (χ_i , χ_e , χ_r , D), while energy confinement time is reduced by 35% as T_e/T_i increases by 25%.

Growth rates and plasma frame frequency for low to intermediate-wavenumber instabilities are calculated with GYRO (Fig. 7) at $\rho=0.65$. Higher $k_{\theta}\rho_s$ growth rates increase [Fig. 7(a)] with T_e/T_i , while for $k_{\theta}\rho_s < 0.5$, there is little change. This reflects increasing turbulence from TEM and ETG modes, which also changes the real frequency, which shows advection in the ion diamagnetic direction for low T_e/T_i and electron direction at higher T_e/T_i .

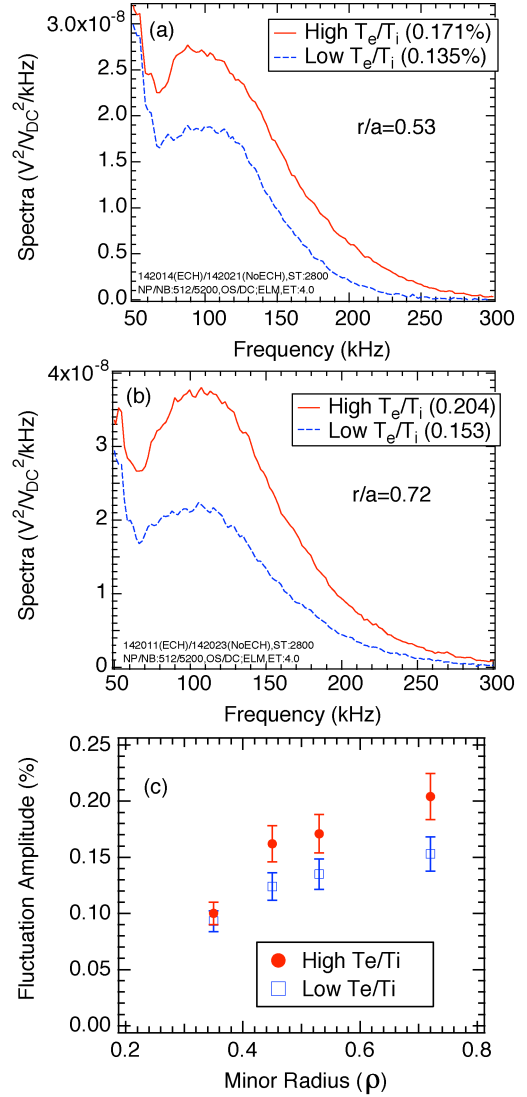


Fig. 6. Turbulence measurements with BES: (a) density fluctuation spectra at $\rho=0.53$ for high T_e/T_i (red) and low T_e/T_i (blue), (b) same at $\rho=0.72$, and (c) profile comparison of fluctuation amplitude.

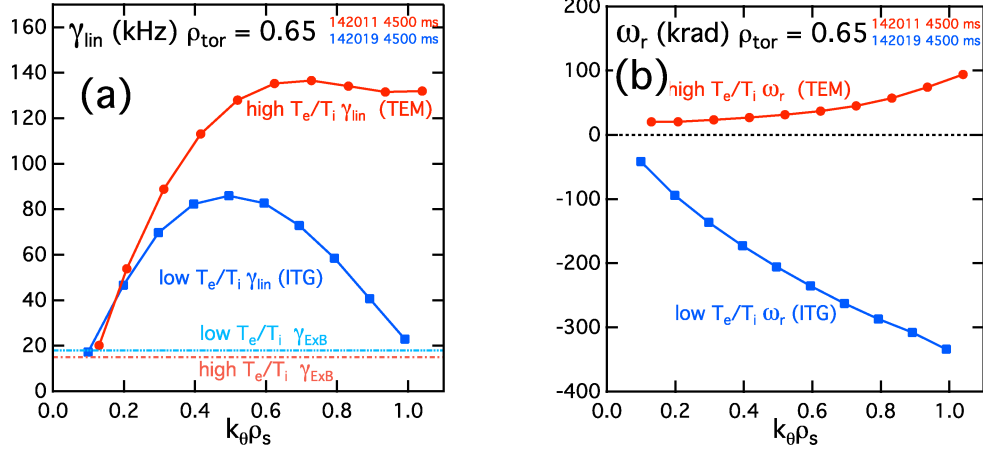


Fig. 7. GYRO calculations of (a) linear growth rates and measured ExB shearing rates, and (b) plasma frame frequencies at $\rho=0.65$ for high and low T_e/T_i plasmas.

4. Discussion and Conclusions

These experiments and analysis establish the turbulence mechanisms, including increases in amplitude and changes in wavenumber, behind transport modifications approaching burning plasma-relevant conditions. These results point towards reduced energy confinement as burning plasma relevant parameters of lower injected torque, and consequently lower rotation and average ExB shear, and near unity T_e/T_i are approached. These initial experiments and comparisons with TGLF and GYRO show generally consistent trends, though some notable discrepancies were identified. Experimental studies will also seek to identify potential mitigating factors that may offset the deleterious effects of low rotation/shear and near unity T_e/T_i , such as the effects of radiative impurities, Shafranov shift and low collisionality.

This material is based upon work supported by the U.S. Department of Energy, Office of Science, Office of Fusion Energy Sciences, using the DIII-D National Fusion Facility, a DOE Office of Science user facility, under Awards DE-FG02-08ER54999, DE-FG02-89ER53296, DE-FG02-07ER54917, DE-FG02-08ER54984, DE-FC02-04ER54698, DE-FG02-04ER54235 and DE-AC02-09CH11466.

References

- [1] T.C. Luce, *et al.*, "Dependence of Confinement and Stability on Variation of the External Torque in the DIII-D Tokamak," Fusion Energy Conference 2006 (Proc. 21st Int. Conf. Chengdu, 2006), IAEA, Vienna (2007), PD-3.
- [2] G.M. Staebler, J.E. Kinsey, R.E. Waltz, *Phys. Plasmas* **14**, 055909 (2007).
- [3] M.R. Wade, *et al.*, *Nucl. Fusion* **45**, 407 (2005).
- [4] K.H. Burrell, *Phys. Plasmas* **4**, 1499 (1997).
- [5] P. Politzer, *et al.*, *Nucl. Fusion* **48**, 075001 (2008).
- [6] G.R. McKee, *et al.*, *Rev. Sci. Instrum.* **81**, 10D741 (2010).
- [7] J.C. Hillesheim, *et al.*, *Rev. Sci. Instrum.* **81**, 10D907 (2010).
- [8] J.R. Dorris, J.C. Rost, M. Porkolab, *Rev. Sci. Instrum.* **80**, 023503 (2009).
- [9] M.W. Shafer, *et al.*, *Phys. Plasmas* **19**, 032504 (2012).
- [10] C. Holland, *et al.*, *Phys. Plasmas* **16**, 052301 (2009).
- [11] C.C. Petty, *et al.*, *Phys. Rev. Lett.* **83**, 3661 (1999).
- [12] J. Stober, *et al.*, "Dominant ECR Heating of H-mode Plasmas on ASDEX-Upgrade," Fusion Energy Conference 2012, EX1/4.